

Smart Placement, Faster Robots – A Comparison of Algorithms for Robot Base-Pose Optimization

Matthias Mayer and Matthias Althoff

Abstract—Robotic automation is a key technology that increases the efficiency and flexibility of manufacturing processes. However, one of the challenges in deploying robots in novel environments is finding the optimal base pose for the robot, which affects its reachability and deployment cost. Yet, the existing research for automatically optimizing the base pose of robots has not been compared. We address this problem by optimizing the base pose of industrial robots with Bayesian optimization, exhaustive search, genetic algorithms, and stochastic gradient descent and find that all algorithms can reduce the cycle time for various evaluated tasks in synthetic and real-world environments. Stochastic gradient descent shows superior performance with regard to success rate solving over 90% of our real-world tasks, while genetic algorithms show the lowest final costs. All benchmarks and implemented methods are available as baselines against which novel approaches can be compared.

Index Terms—Industrial Robots, Methods and Tools for Robot System Design, Performance Evaluation and Benchmarking

I. INTRODUCTION

AN often overlooked factor in the deployment of robots is the positioning of their base, which can substantially improve their performance, usually without additional monetary costs. The trend towards lighter robots also supports a more flexible base pose selection, as these robots need less sturdy foundations. By optimizing the placement of the robot, we can unlock hardware savings by making a robot more productive or by making it possible to use a simpler (modular) robot.

In this paper, we compare algorithms that optimize the base pose of robots to improve their productivity. We focus on methods that do not require significant adaptations to a specific robot, such that they can, in principle, accommodate changing modular robots. Within the literature, we found exhaustive search (ES) [1], gradient-based methods [2], genetic algorithms (GAs) [3], and Bayesian optimization (BO) [4] as the most used methods to optimize robotic base poses. To apply gradient-based methods to arbitrary robots, we adapted Adam [5], a stochastic gradient descent (SGD) method, to base placement optimization. Compared to [2], which assumes a spherical wrist, our SGD only requires a well-defined forward kinematics.

Our evaluation reveals that SGD succeeds significantly more often than other methods in the tasks with the most goals. In contrast, GA significantly lowers cycle times in tasks that force the robot to be placed in one part of the optimization

This work was supported by the Deutsche Forschungsgemeinschaft (German Research Foundation) under grant number AL 1185/31-1.

All authors are with the Technical University of Munich, TUM School of Computation, Information and Technology, Chair of Robotics, Artificial Intelligence and Real-time Systems, Boltzmannstraße 3, 85748, Garching, Germany. {matthias.mayer, althoff}@tum.de

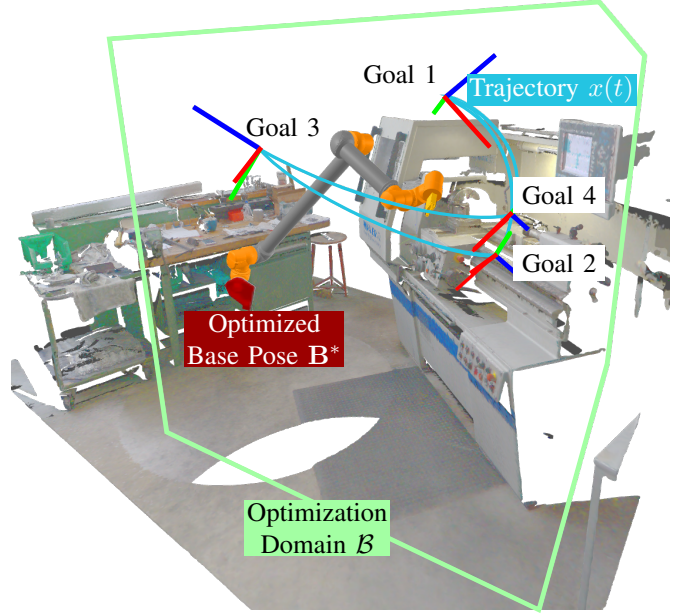


Fig. 1. Visualization of the optimized base pose B^* of robot⁶ R solving a point-to-point movement in a 3D-scanned environment². The trajectory $x(t)$ connects the four goal poses $g_{0..3}$ drawn as coordinate frames. We indicate the allowed base positions of the robot B in 3D space by the green outline of a box.

domain, as shown in Fig. 3. In most cases, BO is significantly outperformed, having the lowest success rate and highest average cycle times. Additionally, we find strong generalization abilities for the fine-tuned algorithms, specifically for the task set containing 3D-scanned environments, as shown in Fig. 1.

A. Related Work

We summarize the state of the art for base placement optimization (BPO) and discuss related and established benchmarks. Optimizing the base pose can be considered part of laying out a manufacturing system. The review in [6] discusses different methods, mostly from derivative-free black-box optimization.

Noticeable exceptions are [2], [7], which formulate base placement optimization as (convex) optimization problems. [2] exploits the fact that the inverse kinematics of industrial robots with spherical wrists can be decomposed into a positioning and orientation sub-problem. [7] optimize the entire robot structure, but specifically the robot base jointly in a trajectory tracking problem. They model the base as a set of zero-velocity joints and solve the whole optimization via collocation.

²Additional information, s.a., animations, and all other best solutions, are available at cobra.cps.cit.tum.de/tools/rbo.

We group the remaining methods into exhaustive search, capability maps, genetic algorithms, and Bayesian optimization:

a) Exhaustive search (ES): This method optimizes the base position of an industrial robot by evaluating all base positions on an equidistant grid [1].

b) Capability maps: Another approach are capability maps as used by [8]–[10]. All of these exploit rather expensive pre-calculations of capability maps for the considered robots, e.g., discretizing the robot workspace into voxels and storing the manipulability at the center of each voxel. These approaches position the robot such that all desired workspace poses lie within areas of high capability.

c) Genetic algorithms (GAs): The authors in [3] use genetic algorithms to jointly optimize the base position and initial guesses for numerical inverse kinematic solutions. The initial inverse kinematic guesses are refined by local search with a quasi-Newton algorithm. A fitness function evaluates the closeness to all desired poses and maximizes manipulability at the desired poses.

Recently, base poses and modular reconfigurable robots have been jointly optimized in [11], [12]. Both encode the base pose as six additional discretized genes for position and orientation and prepend it to the robot module encoding.

d) Bayesian optimization (BO): The work in [4] uses BO to optimize the shoulder placement of the arms of a bimanual humanoid robot. The authors especially highlight the ability to explore and exploit the Pareto front of optimal base poses with regard to a set of different manipulation tasks the robot should fulfill.

e) Benchmarks: The previous base placement optimization algorithms have not yet been compared on a common set of benchmark tasks. In the robotics community, various benchmark suites have helped to select promising algorithms for many related problems. One example is motion planning, where [13, Tab. 1] provides a great overview of available benchmarks. Also, in the area of grasp planning, various benchmark sets and challenges have been proposed, as summarized by [14, p. 1]. Within the area of robotic assembly, challenges such as those run by NIST³ helped make progress in tasks, such as the insertion of various parts and handling of limp objects, e.g., wires and belts. The found benchmarks either excluded the robot base position from the optimization problem [13], [14], focusing on the motion/grasp planning problem, or left the whole system design open (NIST), such that the base optimization cannot be analyzed on its own.

To isolate the base optimization, we use the benchmark suite CoBRA [15], which describes varying robotic *tasks* including motion *goals*, *obstacles* to move around, and *constraints* to obey. Its constraints for the robotic base enable precise definitions of the optimization domain \mathcal{B} while keeping other benchmark components constant. Furthermore, CoBRA defines (modular) robots to solve these tasks with and cost functions to compare them on.

We focus on robotic tasks that require point-to-point movements, as can be found, e.g., in machine tending, (spot)

welding, or dispensing, and was used by [1], [3], [4], [8], [10]. According to [16, p. 13], these still make up the majority of tasks automated by robots ensuring the wide applicability of our approach.

B. Contributions

We present the first work comparing base placement optimization (BPO) algorithms on a set of benchmarks and adapt Adam [5], a stochastic gradient descent (SGD) method, to the BPO problem. In particular, we

- compare BPO methods (GA, BO, ES, and SGD);
- propose benchmarks to compare BPO methods on;
- for the first time apply SGD to the BPO problem;
- test the generalizability of these BPO methods to various tasks and with different allowed base poses;
- systematically tune the hyperparameters of GA, BO, and SGD for BPO.

In Sec. II, we define the optimization problem and introduce the evaluated methods. Sec. III states the setup for our evaluation and summarizes the results. These are discussed in Sec. IV, which is followed by a conclusion in Sec. V.

II. METHODS

This section defines the base placement optimization problem and presents how the considered optimization methods can solve it. We closely follow the notation introduced in CoBRA [15]. In summary, we use lowercase letters for scalars, e.g., $t_f \in \mathbb{R}$, bars to indicate vectors, e.g., $\bar{b} \in \mathbb{R}^N$, uppercase and bold letters for poses, e.g., \mathbf{B} , and calligraphic letters for sets, e.g., \mathcal{G} .

Our robotic tasks are given as a tuple containing a set of goal poses for the end effector \mathcal{G} , a set of constraint functions \mathcal{C} , a set of environment obstacles \mathcal{O} , and a cost function J_C . The set of constraints \mathcal{C} enforces common desired properties, such as respecting the joint limits and avoiding collisions with \mathcal{O} . For each task, a trajectory $x(t)$ and base pose $\mathbf{B} \in SE(3)^4$ need to be found that satisfy all constraints in \mathcal{C} . The trajectory, especially, needs to pass through all goals \mathcal{G} during its execution time t_f , which is ensured by its generation described in Sec. II-E.

Additionally, constraints in \mathcal{C} can limit the range of base poses, which we summarize as a set of valid base poses

$$\mathcal{B} = \{\mathbf{B} \in SE(3) \mid \forall c \in \mathcal{C} : c(x(t), t, \mathbf{B}, R) \leq 0\}. \quad (1)$$

Our paper aims to find the optimal base pose

$$\mathbf{B}^* = \arg \min_{\mathbf{B} \in \mathcal{B}} \left(J_C(R, \mathbf{B}, x(t)) \right). \quad (2)$$

subject to $\forall t \in [0, t_f]$:

$$\forall c \in \mathcal{C} : c(x(t), t, \mathbf{B}, R) \leq 0. \quad (3)$$

For all considered optimizers, we need an a dimensional vector $\bar{b} \in \mathbb{R}^a$ to parameterize \mathbf{B} , where $\bar{b}_{i:j} = [b_i, \dots, b_j]$

³www.nist.gov/el/intelligent-systems-division-73500/robotic-grasping-and-manipulation-assembly/assembly, Accessed: April 23rd, 2025.

⁴ $SE(3) = \mathbb{R}^3 \times SO(3)$ is the space representing an arbitrary pose, i.e., position \mathbb{R}^3 and orientation $SO(3)$ in three-dimensional space. Commonly represented as a 4×4 homogeneous transformation matrix [17, Sec. 2.2.3].

contains the elements i through j from $\bar{b} = [b_1, \dots, b_N]$ and $\bar{0}_N$ is the N -dimensional vector of zeros. We use

- $a = 3$ encoding only the Cartesian position as used, e.g., in [1]:

$$\mathbf{B}_1(\bar{b}) = \begin{bmatrix} \mathbf{1}_{3 \times 3} & \bar{b}_{1:3} \\ \bar{0}_3^T & 1 \end{bmatrix} \quad (4)$$

- $a = 6$ adding an axis angle encoding [17, Tab. 2.1], similar to [11], and extending [3], [4]:

$$\mathbf{B}_2(\bar{b}) = \mathbf{B}_{\text{pos}}(\bar{b}_{1:3}) \begin{bmatrix} \mathbf{R}_{\text{axis-angle}}(\bar{b}_{4:6}) & \bar{0}_3 \\ \bar{0}_3^T & 1 \end{bmatrix} \quad (5)$$

Next, we present the considered optimization approaches.

A. Baseline and Exhaustive Search (ES)

As a baseline, we implement a *dummy* base placement optimization algorithm that keeps the nominal pose provided by the robotic task. Additionally, we consider a *random* optimizer that uniformly samples poses from the allowed set \mathcal{B} . With an increasing number of sampled points, it approximates the ES method surveyed in Sec. I-A.

B. Genetic Algorithms (GAs)

GAs belong to the set of black-box optimization algorithms. Within a GA, a population of individual solution candidates encoded as a list of genes is optimized. Those genes are our parameter vectors defined in (4) and (5) and are altered by:

- mutation, which locally alters a single or several genes of an individual;
- cross-over, which combines genes from two individuals to create a new "offspring";
- selection, which determines how individuals are added to the next generation.

The mutation operator uniformly selects single values $b_i, i \in [1, \dots, a]$ to alter and adds a random number from a scalar normal distribution with zero mean and unit standard deviation $\mathcal{N}(0, 1)$ to them. Cross-over selects the first $n \in [1, \dots, a]$ entries in one gene vector and combines it with the last $a - n$ elements from another individual. The selection is based on the negative cost function $-\mathcal{J}_C(\mathbf{B})$, which is considered the fitness of each individual.

C. Bayesian Optimization (BO)

BO is another common method within derivative-free or black-box optimization algorithms. Following [4], our BO uses Gaussian mixture models $\hat{\mathcal{J}}_C(\mathbf{B})$ to approximate the cost of i previously tested base poses $\{\mathcal{J}_C(\mathbf{B}_1), \dots, \mathcal{J}_C(\mathbf{B}_i)\}$. The next base pose \mathbf{B}_{i+1} to explore is sampled from $\hat{\mathcal{J}}_C$ based on the exploration/exploitation hyperparameter ξ . The resulting cost $\mathcal{J}_C(\mathbf{B}_{i+1})$ can in turn be used to refine $\hat{\mathcal{J}}_C$. For base placement optimization, we define $\hat{\mathcal{J}}_C$ using $\bar{b} \in \mathbb{R}^a$ following (4) and (5). $\hat{\mathcal{J}}_C$ maps to the scalar cost value $\mathcal{J}_C(\mathbf{B})$ and can be used to propose the next base pose \mathbf{B}_{i+1} to test. At the start, BO commonly samples $n_{\text{init}} \in \mathbb{N}_{>0}$ points, e.g., randomly or from low-discrepancy sequences, such as the Hammersley set [18]. The initial sampling method is also determined via hyperparameter tuning.

D. Stochastic Gradient Decent (SGD)

SGD are gradient-based methods that rose to prominence for training deep neural networks. A current state-of-the-art SGD algorithm is Adam [5]. Given a manipulator with known forward kinematics $\text{FK} : \mathbb{R}^N \rightarrow SE(3)$, i.e., a function returning the end-effector pose of a robot given its joint angles $\bar{q} \in \mathbb{R}^N$ and a distance function $\delta : SE(3) \times SE(3) \rightarrow \mathbb{R}_{\geq 0}$, we can use numerical inverse kinematics (IK) to find configurations \bar{q}_i close to desired goal poses g_i [17, Sec. 2.7]. We use Adam to optimize the base pose, such that δ is reduced for the found configurations \bar{q}_i . Starting at a random base pose determined by $\bar{b} \in \mathbb{R}^a$, we can run the following optimization loop $n_{\text{Adam}} \in \mathbb{N}_{>0}$ times:

- 1) Move the robot to $\mathbf{B}(\bar{b})$ and find the closest IK solutions $\bar{q}_i \in \mathbb{R}^N$ to all goals $g_i \in \mathcal{G}$ according to a distance function

$$\delta(\mathbf{B}(\bar{b})\text{FK}(\bar{q}_i), g_i) \geq 0 \quad (6)$$

within a maximum of $n_{\text{IK}} \in \mathbb{N}_{>0}$ steps. Terminate if all IK solutions are within the tolerance of each goal.

- 2) Calculate the gradient of δ with respect to the base parameters \bar{b} at each found IK solution \bar{q}_i :

$$\nabla \delta_i = \frac{\partial \delta(\mathbf{B}(\bar{b})\text{FK}(\bar{q}_i), g_i)}{\partial \bar{b}} \quad (7)$$

- 3) Adam updates \bar{b} based on $\nabla \delta = \sum_{i=0}^{|\mathcal{G}|} \nabla \delta_i$ using an exponential decaying average of $\nabla \delta$ determined by $\beta_1, \beta_2 \in [0, 1)$ and a step size $\alpha > 0$ [5, Alg. 1].

The algorithm is restarted from other random initial guesses as long as there is time left to escape local minima.

E. Task Solver

All base placement optimization methods have access to the same task solver that judges whether a suggested base pose \mathbf{B} allows the robot R to fulfill all goals \mathcal{G} of a given task. This solver first applies step-by-step elimination [19, p. 7-8] to reject base poses further away from any goal than the maximum length of the robot or those without (collision-free) inverse kinematic solutions. If these filters pass, we run RRT-Connect [20] and the trajectory generator proposed in [21] to find a collision-free and feasible trajectory $x(t)$ for the robot positioned at \mathbf{B} . The overall process is summarized in Fig. 2. We calculate the cost function \mathcal{J}_C based on the found trajectory. If any step fails, a fixed failure cost $J_{\text{fail}} \in \mathbb{R}$ is returned to the optimizer.

The overall runtime of the task solver varies depending on which filter rejects the suggested base pose. For reference, a failure in the first two steps can be determined within milliseconds, as these only need a few forward kinematic calculations. Finding collision-free inverse kinematic solutions is done in about one hundred milliseconds, while the path planner succeeds in the order of seconds and only fails after a fixed time-out is reached.

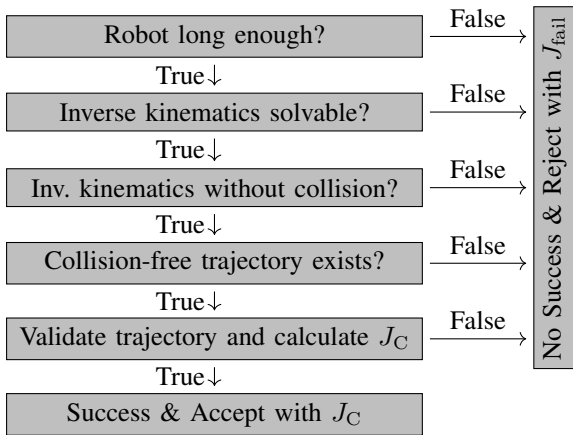


Fig. 2. Order of filters to test if the base pose is feasible and calculate the cost at that pose.

III. NUMERICAL EXPERIMENTS

We ran the following numerical experiments to evaluate and compare the suggested base placement optimization algorithms⁵. First, we present the setup, including the set of considered robotic tasks and specific libraries for implementing the optimizers. Second, we analyze the adaptability, convergence, and generalizability of each approach for various different robotic tasks.

A. Setup

In all our experiments, we use Timor Python [22] for kinematic calculations and collision detection. Our benchmark tasks are implemented as CoBRA tasks [15]. We created our *simple* set of 100 tasks by sampling three cubic obstacles on a grid about the origin and three desired poses outside those cubes that the end effector should stop at, as proposed in [23]. Moreover, we tested the tuned methods on the sets

- *hard*: 100 synthetic tasks using the same sampling as the simple set of tasks with five goals and obstacles instead of three.
- *real*: 27 tasks based on 3D-scanned real-world factory settings in which CNC machines are fed, e.g., Fig. 1.
- *edge*: 100 specifically created cases where goals are all located outside of \mathcal{B} and additionally placed close to obstacles to limit the feasible base poses, such as goal 3 in Fig. 3.

The tasks in each set are listed on² and are tagged with BPO24 and simple/hard/real/edge_case_hard in CoBRA.

All tasks have the following constraints:

- Joints limited in position q and torque τ ,
- no (self-)collisions,
- all goal poses need to be passed, and
- the robot base must be positioned around a given pose with ± 1 m in each Cartesian direction and no limit on orientation.

In all cases, the goal was to minimize the cycle time $J_T = t_f$ in seconds required to fulfill the given task with a given robot⁶. If

⁵ All code is available at gitlab.lrz.de/tum-cps/robot-base-pose-optimization.

⁶Made from the CoBRA module set `mod_rob-gen2` with module order $M = [105, 2, 2, 24, 2, 25, 1, 1, 1, \text{GEP2010IL}]$ and shown in Figs. 1 and 3

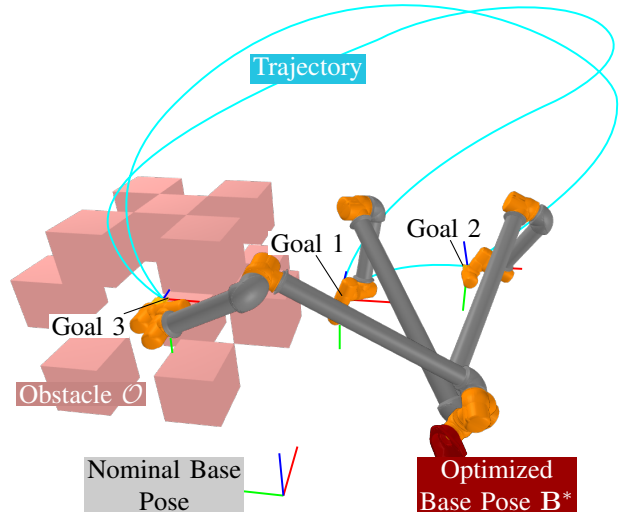


Fig. 3. Example solution of a task from the *edge* set. We show the cubic obstacles \mathcal{O} around goal 3, the robot R solving each goal, and the end-effector trajectory $x(t)$ in cyan. Additionally, all goals \mathcal{G} with their desired pose and the nominal base pose at the center of \mathcal{B} are shown.

the task solver cannot find a solution trajectory for a suggested base pose, a default failure cost of $J_{\text{fail}} = 20$ s is returned, which is well above the possible cycle time. All experiments were run on a 64-core AMD EPYC 7742 clocked at 2.25 GHz.

We used Adam and automatic differentiation provided by PyTorch 2.2.1 [24] to implement SGD, and the GA optimizer was implemented with PyGAD [25]. BO used the implementation provided by scikit-optimize⁷. SGD, GA and BO require setting hyperparameters to tune them for specific applications, in contrast to *dummy* and *random*. We used Optuna [26] in its default setting with the Tree-structured Parzen Estimator (TPE) optimizer [27] and median pruner to minimize the mean cost on the first 70% of simple tasks. The base placement optimization was limited to finding the best position for the robot base, i.e., using (4). In total, we ran 400 trials for each of the three tunable algorithms with Optuna. The optimized hyperparameters are listed in Tab. I. For ES, we did not identify any tunable parameter; it always uses a uniform distribution sampling from the whole domain of \bar{b} .

The final comparison of tuned algorithms occurred on a distinct set of tasks not used during hyperparameter optimization, i.e., the last 30% of the simple set and the complete sets hard, real, and edge. For all sets besides simple, we had to increase the failure penalty to $J_{\text{fail}} = 50$ s, as the additional goals and more complex obstacles need, on average, longer cycle times. The comparison with tasks from the simple set allows us to judge the performance of each algorithm, while comparison with the tasks from other sets shows generalization potential. Algorithms are compared in a fixed-budget setting: they get $t_{\text{CPU}} = 1200$ s = 20 min⁸ per task to explore possible base poses by running the provided filters and, on success, complete

⁷scikit-optimize.github.io/stable/modules/generated/skopt.Optimizer.html, Accessed: April 23rd, 2025.

⁸Set by preliminary tests on the simple set, which showed convergence after this optimization time.

TABLE I
OPTIMIZED HYPERPARAMETERS

Stochastic gradient descent (SGD) [24]		Genetic algorithm (GA) [25]		Bayesian optimization (BO) ⁷	
Learning rate α	0.3923	Population Size	25	Acquisition Func.	Expected Improvement
Momentum decay β_1	0.8749	Mutation Prob.	0.2690	Acquisition Optim.	Sampling
Momentum decay β_2	0.9739	#Parents Mating	14	Batch Size	1
Adam steps n_{Adam}	44	Keep Parents	12	Initial Point Gen.	Hammersly
Inv. kin. steps n_{IK}	33	Crossover Type	Single Point	#Initial Points n_{init}	31
		Keep Elites	3	Des. Improvement ξ	0.0973

path planning. Both the selection of the next base pose and their evaluation count towards the time budget. The final score is the cost of the best solution, and we present statistics over five distinct seeds.

B. Results

First, we present the convergence of the minimum cost found (top) and the success rate (bottom) on the hard (Fig. 4a) and real set of tasks (Fig. 4b). The success rate is the fraction of tasks and seeds for which each base placement optimization algorithm can find a valid base pose within the optimization time given on the x-axis. The first column of each subfigure evaluates the same setting (4) used during hyperparameter optimization, only optimizing the base position; the second column uses (5) to optimize the position and orientation. The mean and 95% confidence interval calculated via bootstrapping over all tasks and seeds are shown for each method.

Second, we summarize the final average best cycle time and the success rate of each method on all sets of tasks in Tab. II. To judge significance, we provide the mean expected cost/success rate, and 95% confidence intervals of each found via bootstrapping. Therefore, the numbers provided in Tab. II for the hard task set show the mean and confidence interval at t_{CPU} from Fig. 4a. Mean values significantly *worse* or **better** than all others are highlighted, i.e., mean values outside the confidence interval of all other methods in the same row. The hard, real, and edge sets of tasks test generalization, as they have different distributions of goal poses and obstacles compared to the simple set of tasks used for hyperparameter optimization. We omit the *dummy* optimizer, as it can only solve the simple set of tasks in 47% of cases and the hard set of tasks in 18% while failing to solve any task from the other sets.

IV. DISCUSSION

With regard to overall performance, we find that all algorithms outperform the *dummy* optimizer, highlighting that base pose optimization can significantly decrease cycle time. Moreover, all methods constantly show noticeable confidence intervals in Fig. 4 and Tab. II due to the stochasticity of the evaluated approaches and the underlying trajectory generation process (see Sec. II-E). The time limit of 1200 s seems enough for the simple and real set of tasks, as evidenced by the success rate plateauing in Fig. 4b. The edge and hard set of tasks could improve with more computation time, as their success rates have not leveled off.

The state-of-the-art methods (GA, BO, *random*) perform quite similarly on the hard and real task sets and in either optimization domain, as plotted in Fig. 4. However, in the end, BO often performs significantly worse than the other methods, as indicated by the *italic means* outside the other confidence intervals in Tab. II. Looking at the average best cost at the end of the runtime, GA seems to have a slight edge over existing methods with significantly lower cost on the set of tasks edge (**bold** in Tab. II upper half) and the lowest average in all other cases. With regard to success rate, our adaptation of SGD is significantly better in three settings (**bold** in Tab. II lower half) and shows the highest average in the other settings. It also increases the success rate faster than the other methods in three out of four cases in Fig. 4.

Concerning generalization to sets of tasks not used for hyperparameter parameterization, all algorithms experienced significant losses in success rate, i.e., the mean success rates in each column are outside the confidence interval for the simple set of tasks. Still, for the real set of tasks, we find success rates of over 80% with all algorithms. On average, SGD is the most successful on the real set of tasks with over 90% success rate, a significant improvement over *random* and GA.

Benefits from the bigger optimization domain of position and orientation are not realized by all methods on all sets of tasks. Looking at the success rate in Tab. II, in the hard and real sets, we see *random* and BO deteriorating while GA improves its performance (all non-significantly). Additionally, Tab. II shows that for the edge set of tasks, the bigger search space significantly increases the success rate with all methods. Lastly, the bigger search space also often decreases final cycle time, e.g., in three of four cases for SGD and GA.

V. CONCLUSION

For the first time, this paper compares existing robot base pose optimizers, namely Bayesian optimization (BO), exhaustive search (ES), and genetic algorithms (GAs), focusing on methods needing no pre-calculations. Also, for the first time, we apply Adam, a stochastic gradient descent (SGD)-based optimizer, to this problem. Each algorithm was implemented in an anytime fashion, allowing the user to set a time budget for finding the best base pose. The hyperparameters of each method were optimized, and the methods were compared on a set of diverse robotic tasks, both synthetic and based on real-world 3D scans.

The three previously applied methods (BO, ES, GA) showed comparable success rates on our simple set of tasks, but with

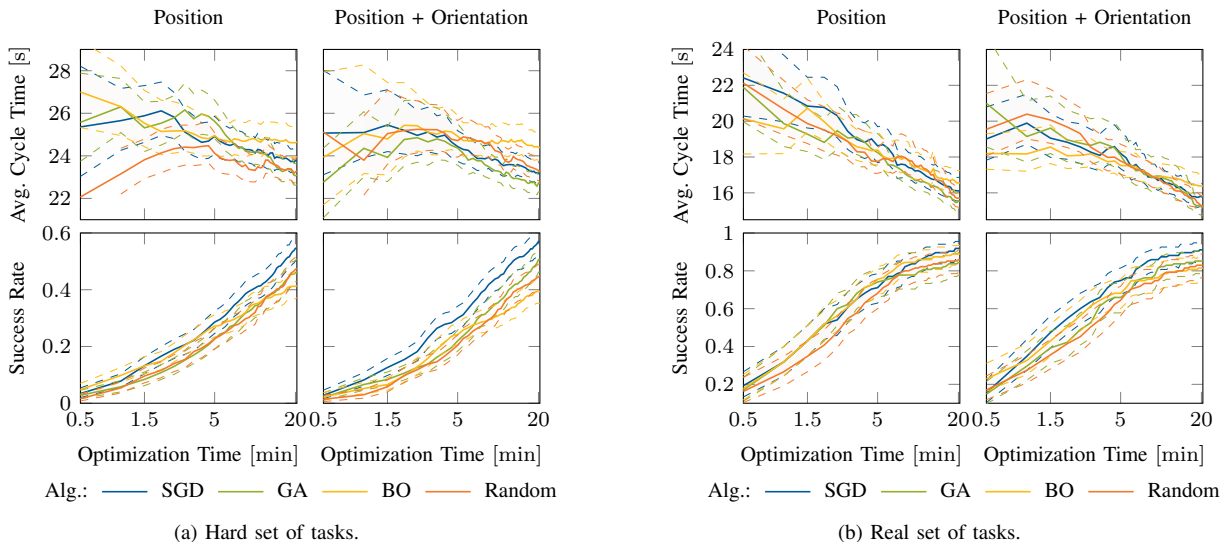


Fig. 4. The best found cost (top) and rate of success (bottom) over the optimization time (x-axis), for the four algorithms (color) optimizing the position (left) or position + orientation (right) on the noted set of tests. Each plot shows the mean — and edges - - - of their 95 % confidence intervals.

TABLE II

THE MEAN AND 95 % CONFIDENCE INTERVAL (CI) FOR THE SUCCESS RATE BEST FOUND CYCLE TIME. ARROWS \uparrow , \downarrow INDICATE THE DIRECTION OF BETTER VALUES. HIGHLIGHTED MEANS ARE SIGNIFICANT, I.E., *WORSE* OR *BETTER* THAN ANY OTHER CI.

Measurement	Action Space	Task Set	Random	GA	BO	SGD
\downarrow Average Best Cycle Time s	Position	Simple	10.77 [10.50, 11.15]	10.69 [10.41, 11.08]	<i>11.37</i> [11.10, 11.73]	10.81 [10.54, 11.20]
		Hard	23.29 [22.78, 23.93]	23.09 [22.64, 23.64]	<i>24.65</i> [23.98, 25.42]	23.77 [23.26, 24.36]
		Real	15.70 [15.20, 16.24]	15.53 [15.05, 16.08]	16.55 [15.95, 17.24]	16.11 [15.54, 16.86]
		Edge	15.97 [15.11, 17.14]	13.65 [12.98, 15.44]	<i>18.13</i> [16.23, 22.02]	16.26 [15.28, 17.48]
	Position + Rotation	Simple	10.84 [10.57, 11.22]	10.67 [10.42, 11.08]	<i>11.26</i> [10.97, 11.64]	10.74 [10.47, 11.13]
		Hard	23.28 [22.80, 23.87]	22.71 [22.30, 23.26]	<i>24.40</i> [23.78, 25.09]	23.11 [22.66, 23.63]
		Real	15.28 [14.86, 15.82]	15.22 [14.75, 15.77]	16.38 [15.85, 17.04]	15.74 [15.19, 16.47]
		Edge	15.64 [15.16, 16.21]	14.28 [13.90, 14.70]	<i>17.61</i> [16.78, 18.65]	16.34 [15.78, 17.00]
\uparrow Success Rate %	Position	Simple	96.67 [92.67, 98.67]	96.67 [92.67, 98.67]	96.67 [92.67, 98.67]	96.67 [92.67, 98.67]
		Hard	47.40 [43.00, 51.80]	46.40 [42.00, 50.80]	<i>41.40</i> [37.20, 45.80]	54.60 [50.20, 59.00]
		Real	85.93 [79.26, 91.11]	84.44 [77.78, 89.63]	88.89 [82.96, 93.33]	91.85 [85.93, 95.56]
		Edge	14.60 [11.80, 18.00]	13.80 [11.00, 17.00]	<i>5.40</i> [3.60, 7.60]	15.00 [12.00, 18.40]
	Position + Rotation	Simple	96.67 [92.67, 98.67]	96.67 [92.67, 98.67]	96.67 [92.67, 98.67]	96.67 [92.67, 98.67]
		Hard	44.80 [40.40, 49.00]	50.60 [46.20, 55.00]	<i>39.40</i> [35.20, 43.60]	57.00 [52.80, 61.20]
		Real	82.96 [76.30, 88.89]	85.19 [78.52, 90.37]	81.48 [74.07, 87.41]	91.11 [85.19, 94.81]
		Edge	54.40 [50.20, 58.67]	55.20 [50.80, 59.60]	<i>25.00</i> [21.40, 29.00]	55.40 [51.00, 59.80]

the considered optimization time BO found significantly worse cycle times and GA found on average the best. The novel applied optimizer SGD showed an improved success rate, i.e., it found valid solutions in significantly more trials. It especially outperformed the other methods in complex robotic tasks within cluttered real-world environments or tasks with more goals and obstacles. In the tasks based on real-world 3D scans, over 90% could be solved with SGD, which significantly outperformed the other methods. Additionally, allowing any orientation significantly increases the success rate in our novel set of tasks *edge*, indicating that additional mounting effort benefits more complex tasks.

ACKNOWLEDGEMENTS

We thank Jonathan K ulz for Timor-python, and our students Friedrich Dang, Hao Gao, Lukas Seitz, Matthias Pouleau, Seok

Jung, and Tom Tschigfrei who tested several related ideas.

REFERENCES

- [1] T. Lechler, G. Krem, M. Metzner, M. Sjarov, and J. Franke, "Simulation-based robot placement using a data farming approach," in *Production at the leading edge of technology*, 2021, pp. 419–428.
- [2] S. W. Son and D. S. Kwon, "A convex programming approach to the base placement of a 6-DOF articulated robot with a spherical wrist," *Int. J. Adv. Manuf. Technol.*, vol. 102, pp. 3135–3150, 2019.
- [3] S. Mitsi, K.-D. Bouzakis, D. Sagrais, and G. Mansour, "Determination of optimum robot base location considering discrete end-effector positions by means of hybrid genetic algorithm," *Robot. Comput.-Integr. Manuf.*, vol. 24, no. 1, pp. 50–59, 2008.
- [4] Y. Kim, Z. Pan, and K. Hauser, "MO-BBO: Multi-objective bilevel Bayesian optimization for robot and behavior co-design," in *Proc. of the IEEE Int. Conf. on Robotics and Automation (ICRA)*, 2021, pp. 9877–9883.
- [5] D. P. Kingma and J. Ba, "Adam: A method for stochastic optimization," in *3rd Int. Conf. on Learning Representations ICLR*, 2015.

- [6] G. Moslemipour, T. S. Lee, and D. Rilling, "A review of intelligent approaches for designing dynamic and robust layouts in flexible manufacturing systems," *Int. J. Adv. Manuf. Technol.*, vol. 60, pp. 11–27, 2012.
- [7] J. Baumgärtner, A. Puchta, and J. Fleischer, "One Problem, One Solution: Unifying Robot Design and Cell Layout Optimization," in *IEEE/RSJ Int. Conf. on Intelligent Robots and Systems (IROS)*, 2024, pp. 2292–2298.
- [8] G. Boschetti, R. Rosa, and A. Trevisani, "Optimal robot positioning using task-dependent and direction-selective performance indexes: General definitions and application to a parallel robot," *Robot. Comput.-Integr. Manuf.*, vol. 29, no. 2, pp. 431–443, 2013.
- [9] Y. Lin, H. Zhao, and H. Ding, "Posture optimization methodology of 6R industrial robots for machining using performance evaluation indexes," *Robot. Comput.-Integr. Manuf.*, vol. 48, pp. 59–72, 2017.
- [10] A. Makhmal and A. K. Goins, "Reuleaux: Robot base placement by reachability analysis," in *Proc. of the IEEE Int. Conf. on Robotic Computing (IRC)*, 2018, pp. 137–142.
- [11] E. Romiti, F. Iacobelli, M. Ruzzon, N. Kashiri, J. Malzahn, and N. Tsagarakis, "An Optimization Study on Modular Reconfigurable Robots: Finding the Task-Optimal Design," in *Proc. of the IEEE Int. Conf. on Automation Science and Engineering (CASE)*, 2023, pp. 1–8.
- [12] M. Lei, E. Romiti, A. Laurenz, and N. G. Tsagarakis, "Task-Driven Computational Framework for Simultaneously Optimizing Design and Mounted Pose of Modular Reconfigurable Manipulators," in *IEEE/RSJ Int. Conf. on Intelligent Robots and Systems (IROS)*, 2024, pp. 4563–4570.
- [13] C. Chamzas *et al.*, "MotionBenchMaker: A tool to generate and benchmark motion planning datasets," *IEEE Robot. and Automat. Lett.*, vol. 7, no. 2, pp. 882–889, 2022.
- [14] J. Mahler *et al.*, "Learning ambidextrous robot grasping policies," *Sci. Robot.*, vol. 4, no. 26, 2019.
- [15] M. Mayer, J. Külz, and M. Althoff, "CoBRA: A composable benchmark for robotics applications," in *Proc. of the IEEE Int. Conf. on Robotics and Automation (ICRA)*, 2024, pp. 17 665–17 671.
- [16] IFR International Federation of Robotics, *Presentation of World Robotics 2024*. VDMA Robotics + Automation, 2024.
- [17] B. Siciliano and O. Khatib, *Springer Handbook of Robotics*. Springer, 2016.
- [18] T.-T. Wong, W.-S. Luk, and P.-A. Heng, "Sampling with hammersley and halton points," *Journal of Graphics Tools*, vol. 2, no. 2, pp. 9–24, 1997.
- [19] M. Althoff, A. Giusti, S. B. Liu, and A. Pereira, "Effortless creation of safe robots from modules through self-programming and self-verification," *Sci. Robot.*, vol. 4, no. 31, 2019.
- [20] J. J. Kuffner and S. M. La Valle, "RRT-Connect: An efficient approach to single-query path planning," *Proc. - IEEE Int. Conf. Robot. Autom.*, vol. 2, pp. 995–1001, 2000.
- [21] T. Kunz and M. Stilman, "Time-optimal trajectory generation for path following with bounded acceleration and velocity," in *Robotics: Science and Systems*, 2012, pp. 209–216.
- [22] J. Külz, M. Mayer, and M. Althoff, "Timor Python: A toolbox for industrial modular robotics," in *Proc. of the IEEE/RSJ Int. Conf. on Intelligent Robots and Systems (IROS)*, 2023, pp. 424–431.
- [23] J. Whitman, R. Bhirangi, M. Travers, and H. Choset, "Modular robot design synthesis with deep reinforcement learning," in *Proc. of the AAAI Conf. on Artificial Intelligence (AAAI)*, 2020, pp. 10 418–10 425.
- [24] A. Paszke *et al.*, "PyTorch: An imperative style, high-performance deep learning library," in *Advances in Neural Information Processing Systems (NeurIPS)*, 2019, pp. 8024–8035.
- [25] A. F. Gad, "PyGAD: An intuitive genetic algorithm Python library," *Multimedia Tools and Applications*, pp. 1–14, 2023.
- [26] T. Akiba, S. Sano, T. Yanase, T. Ohta, and M. Koyama, "Optuna: A next-generation hyperparameter optimization framework," in *Proc. - Int. Conf. Knowl. Discov. and Data Mining*, 2019, pp. 2623–2631.
- [27] J. Bergstra, R. Bardenet, Y. Bengio, and B. Kégl, "Algorithms for hyperparameter optimization," in *Proc. of the Int. Conf. on Neural Information Processing Systems (NeurIPS)*, 2011.